Spectral study of the stimulated emission of Nd^{3+} in fluorotellurite bulk glass

A. Miguel,[1] J. Azkargorta,[1] R. Morea,[2] I. Iparraguirre,[1] J. Gonzalo,[2] J. Fernandez,[1,3] and R. Balda[1,3,*]

[1]Departamento de Física Aplicada I, Escuela Superior de Ingeniería, Universidad del País Vasco UPV/EHU, Alda. *Urquijo s/n 48013 Bilbao, Spain*

[2]*Instituto de Optica, Consejo Superior de Investigaciones Científicas CSIC, Serrano 121, 28006 Madrid, Spain*

[3]Materials Physics Center CSIC-UPV/EHU and Donostia International Physics Center, 20018 *San Sebastian, Spain*

[*]*wupbacrr@bi.ehu.es*

Abstract: In this work we present, for the first time to our knowledge, laser emission under wavelength selective laser-pulsed pumping in Nd^{3+}-doped TeO_2-ZnO-ZnF_2 bulk glass for two different Nd^{3+} concentrations. The fluorescence properties of Nd^{3+} ions in this matrix which include, Judd-Ofelt calculation, stimulated emission cross-section of the laser transition and lifetimes are also presented. The site-selective emission and excitation spectra along the $^4I_{9/2}\rightarrow{}^4F_{3/2}$ absorption band show the inhomogeneous behaviour of the crystal field felt by Nd^{3+} ions in this fluorotellurite glass which allows for spectral tuning of the laser output pulse as a function of the pumping wavelength. The emission cross-section obtained from the Judd-Ofelt analysis and spectral data ($4.9x10^{-20}$ cm^2) is in fairly good agreement with the value obtained from the analysis of the laser threshold data ($4x10^{-20}$ cm^2).

OCIS codes: (140.3530) Lasers, neodymium; (300.6500) Spectroscopy, time-resolved; (160.5690) Rare-earth-doped materials.

References and links

1. J. H. Campbell and T. I. Suratwala, "Nd-doped phosphate glasses for high-energy/high-peak-power Lasers," J. Non-Cryst. Solids **263**(264), 318–341 (2000).
2. R. R. Petrin, M. L. Kliewer, J. T. Beasley, R. C. Powell, I. D. Aggarwal, and R. C. Ginther, "Spectroscopy and laser operation of Nd:ZBAN glass," IEEE J. Quantum Electron. **27**(4), 1031–1038 (1991).
3. J. Azkargorta, I. Iparraguirre, R. Balda, J. Fernández, E. Dénoue, and J. L. Adam, "Spectroscopic and Laser Properties of Nd^{3+} in BIGaZLuTMn Fluoride Glass," IEEE J. Quantum Electron. **30**(8), 1862–1867 (1994).
4. J. Azkargorta, I. Iparraguirre, R. Balda, and J. Fernández, "On the origin of bichromatic laser emission in Nd^{3+}-doped fluoride glasses," Opt. Express **16**(16), 11894–11906 (2008).
5. T. Schweizer, D. W. Hewak, D. N. Payne, T. Jensen, and G. Huber, "Rare-earth doped chalcogenide glass laser," Electron. Lett. **32**(7), 666–667 (1996).
6. D. F. de Sousa, L. A. O. Nunes, J. H. Rohling, and M. L. Baesso, "Laser emission at 1077 nm in Nd^{3+}-doped calcium aluminosilicate glass," Appl. Phys. B **77**(1), 59–63 (2003).
7. J. Fernandez, I. Iparraguirre, R. Balda, J. Azkargorta, M. Voda, and J. M. Fernandez-Navarro, "Laser action and upconversion of Nd^{3+} in lead-niobium-germanate bulk glass," Opt. Mater. **25**(2), 185–191 (2004).
8. N. Lei, B. Xu, and Z. H. Jiang, "Ti-sapphire laser pumped Nd-tellurite glass laser," Opt. Commun. **127**(4-6), 263–265 (1996).
9. I. Iparraguirre, J. Azkargorta, J. M. Fernández-Navarro, M. Al-Saleh, J. Fernández, and R. Balda, "Laser action and upconversion of Nd^{3+} in tellurite bulk glass," J. Non-Cryst. Solids **353**(8-10), 990–992 (2007).
10. H. Kalaycioglu, H. Cankaya, G. Ozen, L. Ovecoglu, and A. Sennaroglu, "Lasing at 1065 nm in bulk Nd^{3+}-doped telluride-tungstate glass," Opt. Commun. **281**(24), 6056–6060 (2008).
11. J. S. Wang, E. M. Vogel, and E. Snitzer, "Tellurite glass: a new candidate for fiber devices," Opt. Mater. **3**(3), 187–203 (1994).
12. R. A. H. El-Mallawany, *Tellurite Glasses Handbook-Physical Properties and Data*, (CRC Boca Raton, FL 2001).
13. A. Jha, S. Shen, and M. Naftaly, "Structural origin of spectral broadening of 1.5-μm emission in Er^{3+} doped tellurite glasses," Phys. Rev. B **62**(10), 6215–6227 (2000).
14. M. J. Weber, "Science and technology of laser glass," J. Non-Cryst. Solids **123**(1-3), 208–222 (1990).
15. D. L. Sidebottom, M. A. Hruschka, B. G. Potter, and R. K. Brow, "Structure and optical properties of rare-earth-doped zinc oxyhalide tellurite glasses," J. Non-Cryst. Solids **222**, 282–289 (1997).

#185214 - $15.00 USD Received 11 Feb 2013; revised 4 Apr 2013; accepted 4 Apr 2013; published 8 Apr 2013

16. D. L. Sidebottom, M. A. Hruschka, B. G. Potter, and R. K. Brow, "Increased radiative lifetime of rare earth-doped zinc oxyhalide tellurite glasses," Appl. Phys. Lett. **71**(14), 1963–1965 (1997).
17. V. Nazabal, S. Todoroki, A. Nukui, T. Matsumoto, S. Suehara, T. Hondo, T. Araki, S. Inoue, C. Rivero, and T. Cardinal, "Oxyfluoride tellurite glasses doped with erbium: thermal analysis, structural organization and spectral properties," J. Non-Cryst. Solids **325**(1-3), 85–102 (2003).
18. B. R. Judd, "Optical absorption intensities of rare-earth ions," Phys. Rev. **127**(3), 750–761 (1962).
19. G. S. Ofelt, "Intensities of crystal spectra of rare-earth ions," J. Chem. Phys. **37**(3), 511–520 (1962).
20. R. Rolli, K. Wachtler, M. Wachtler, M. Bettinelli, A. Speghini, and D. Ajò, "Optical Spectroscopy of lanthanide ions in ZnO-TeO_2 glasses," Spectrochim. Acta A Mol. Biomol. Spectrosc. **57**(10), 2009–2017 (2001).
21. K. U. Kumar, V. A. Prathyusha, P. Babu, C. K. Jayasankar, A. S. Joshi, A. Speghini, and M. Bettinelli, "Fluorescence properties of Nd^{3+}-doped tellurite glasses," Spectrochim. Acta A Mol. Biomol. Spectrosc. **67**(3-4), 702–708 (2007).
22. R. R. Jacobs and M. J. Weber, "Dependence of the $^4F_{3/2} \rightarrow {}^4I_{11/2}$ Induced-Emission Cross Section for Nd^{3+} on Glass Composition," IEEE J. Quantum Electron. **QE-10**, 102–111 (1976).
23. E. Nakazawa, "Fundamentals of luminescence," in *Phosphor Handbook,* W. M. Yen, S. Shionoya, and H. Yamamoto, ed. (CRC Press, Boca Raton FL, 2007).
24. M. Inokuti and F. Hirayama, "Influence of Energy Transfer by the Exchange Mechanism on Donor Luminescence," J. Chem. Phys. **43**(6), 1978–1990 (1965).
25. F. Batalioto, D. F. de Sousa, M. J. V. Bell, R. Lebullenger, A. C. Hernandes, and L. A. O. Nunes, "Optical measurements of Nd^{3+}/Yb^{3+} codoped fluorindogallate glasses," J. Non-Cryst. Solids **273**(1-3), 233–238 (2000).
26. R. Balda, J. Fernández, M. A. Arriandiaga, and J. M. Fernández -Navarro, "Spectroscopy and frequency upconversion in Nd^{3+}-doped TeO_2-TiO_2-Nb_2O_5 glass," J. Phys. C.: Condens. Matter **19**(8), 086223–086234 (2007).
27. W. Ryba-Romanowski, S. Golab, L. Cichosz, and B. Jezowska-Trzebiatowska, "Influence of temperature and acceptor concentration on energy transfer from Nd^{3+} to Yb^{3+} and from Yb^{3+} to Er^{3+} in tellurite glass," J. Non-Cryst. Solids **105**(3), 295–302 (1988).
28. I. Iparraguirre, J. Azkargorta, R. Balda, K. Venkata Krishnaiah, C. K. Jayasankar, M. Al-Saleh, and J. Fernández, "Spontaneous and stimulated emission spectroscopy of a Nd^{3+}-doped phosphate glass under wavelength selective pumping," Opt. Express **19**(20), 19440–19453 (2011).

1. Introduction

Neodymium doped glasses have been largely investigated since neodymium has been recognized as one of the most efficient rare-earth ions for solid-state lasers due to its intense $^4F_{3/2} \rightarrow {}^4I_{11/2}$ emission at around 1.06 μm [1]. Until now, neodymium-doped silicate and phosphate-based bulk glasses have been the most widely used laser glasses due to their good optical, thermal, and mechanical properties. Laser emission has also been obtained in other bulk glasses doped with Nd^{3+} such as fluorides [2–4], chalcogenides [5], aluminosilicates [6], germanates [7], and tellurite glasses [8–10].

The development of Nd-doped materials for laser applications requires hosts with a low phonon frequency and a low content of OH groups to minimize the multiphonon relaxation rates to enhance the quantum efficiency of emitting levels. Among oxide glasses, TeO_2-based glasses combine good mechanical stability, chemical durability, high linear, and nonlinear refractive indices, together with low phonon energies (~750 cm^{-1}) with a wide transmission window (typically 0.4-6 μm) and high rare-earth solubility [11–13]. The low phonon energy reduces the multiphonon relaxation rates and increases the quantum efficiency of the $^4F_{3/2} \rightarrow {}^4I_{11/2}$ emission of Nd^{3+}. Furthermore, the relatively high values of the refractive index ($1.8<n<2.3$) [11, 12] lead to large stimulated emission cross-sections [14]. The stimulated emission cross-sections of Nd^{3+} for some tellurite glasses obtained by the Judd-Ofelt (JO) approximation are even larger than for phosphate glasses due to the large refractive index [14]. On the other hand, the presence of fluorine ions which can release hydrogen species and reduce the OH content has a great influence in the quenching processes of the radiative emission of excited levels of rare-earth ions.

Zinc tellurite binary glasses have shown interesting properties for photonic applications [15, 16]. Besides, it was found that the partial substitution of ZnO with ZnF_2 significantly expands the glass forming range of the zinc tellurite system and increases the radiative lifetime of rare-earth ions [15–17].

In this work we present, for the first time to our knowledge, laser emission under wavelength selective laser-pulsed pumping in Nd^{3+}-doped TeO_2-ZnO-ZnF_2 bulk glasses for two different NdF_3 concentrations (1 and 2 wt%). The crystal field inhomogeneity produced

#185214 - $15.00 USD Received 11 Feb 2013; revised 4 Apr 2013; accepted 4 Apr 2013; published 8 Apr 2013

by the glass matrix allows for spectral tuning of the laser output pulse. The fluorescence properties of Nd^{3+} ions in this matrix which include Judd-Ofelt calculation, emission peak wavelength, stimulated emission cross-section of the laser transition and lifetimes, together with the results of site-selective laser spectroscopy by exciting along the $^4I_{9/2} \rightarrow {}^4F_{3/2}$ absorption band, are also presented. The excitation spectra show the existence of a variety of crystal field site distributions for Nd^{3+} ions in this glass. Moreover, the spectral shift and narrowing observed in the steady-state emission spectra of the $^4F_{3/2} \rightarrow {}^4I_{11/2}$ transition under selective excitation along the $^4I_{9/2} \rightarrow {}^4F_{3/2}$ absorption band, reveal the existence of a variety of spectrally isolated distributions of Nd^{3+} sites in this glass which is in the origin of the spectral tuning of the laser output pulse.

2. Experimental techniques

Fluorotellurite glasses having a nominal composition of $74.6TeO_2$–$8.8ZnO$–$16.6ZnF_2$ mol% were prepared by mixing the corresponding high purity (99.99%) oxides and fluorides (TeO_2, ZnO, ZnF_2 and NdF_3) in an agate balls mill. The powder mixture was melted in a covered platinum crucible using an electrical vertical furnace at temperatures in the 800–850 °C range. Glass melts were homogenised by using an electrical platinum stirrer and after 20 min the glasses were poured onto a preheated brass mould. The obtained glass blocks (about 1 cm^3 size) were immediately introduced into the annealing furnace, kept for 10 min at temperatures ranging from 300 to 320 °C, and then cooled down to room temperature. The glass was doped with 1 and 2 wt% (0.7 and 1.4 mol% respectively) concentrations of NdF_3. The optical measurements were carried out on polished planoparallel glass slabs of about 1 mm thickness.

Conventional absorption spectra were performed with a Cary 5 spectrophotometer. The samples temperature was varied between 10 and 300 K in a continuous flow cryostat. Site-selective steady-state emission and excitation spectra were obtained by exciting the samples with a continuous wave (cw) Ti-sapphire ring laser (0.4 cm^{-1} linewidth) in the 780-920 nm spectral range. The fluorescence was analyzed with a 0.25 m monochromator equipped with a 1200 lines/mm diffraction grating, and the signal was detected by a Hamamatsu R5509-72 photomultiplier and finally amplified by a standard lock-in technique. The attained resolution was 0.1 nm.

Lifetime measurements were obtained by exciting the samples with a pulsed Ti-sapphire laser (10 ns pulse width) pumped by a pulsed frequency doubled Nd:YAG laser, and detecting the emission with a Hamamatsu R5509-72 photomultiplier and a Tektronix oscilloscope. Data were processed in a personal computer.

3. Results and discussion

3.1 Absorption and emission properties

The room-temperature absorption spectra were recorded in the 300-2500 nm spectral range by using a Cary 5 spectrophotometer. Figure 1 shows the room temperature absorption cross-section as a function of wavelength in the 350-950 nm spectral range. The inhomogeneously broadened bands are assigned to the transitions from the $^4I_{9/2}$ ground state to the excited states of Nd^{3+} ions. Energy levels above $^2P_{1/2}$ are not observed because of the intrinsic bandgap absorption in the host glass.

#185214 - $15.00 USD Received 11 Feb 2013; revised 4 Apr 2013; accepted 4 Apr 2013; published 8 Apr 2013

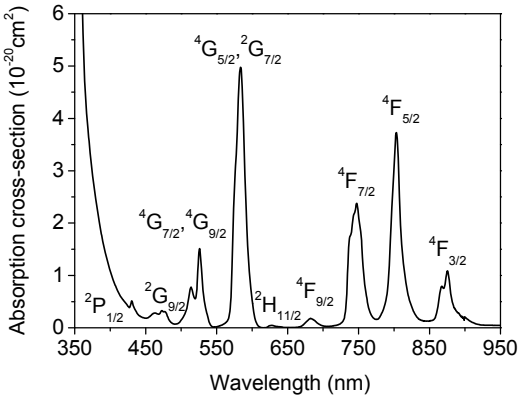

Fig. 1. Room temperature absorption cross-section of Nd^{3+} ions in TeO_2-ZnO-ZnF_2 glass.

The absorption bands in Fig. 1 have been used to calculate the radiative lifetime of the $^4F_{3/2}$ excited state, the branching ratios, and the radiative transition probabilities of fluorescence transitions to the lower lying ^4I_J manifold, according to the Judd-Ofelt theory [18, 19]. The JO parameters obtained for this glass are $\Omega_2 = 3.11\text{x}10^{-20}$ cm^2, $\Omega_4 = 5.00\text{x}10^{-20}$ cm^2, and $\Omega_6 = 3.87\text{x}10^{-20}$ cm^2, with a root-mean-squared deviation equal to $6.03\text{x}10^{-7}$. The values of the JO parameters are in the usually observed range for tellurite glasses. However, the presence of ZnF_2 in this glass, which favors the presence of fluorine ions around Nd^{3+}, decreases the covalency degree in the rare-earth site and results in a lower value of Ω_2 if compared with zinc tellurite glasses [20, 21].

The $^4F_{3/2}\rightarrow{}^4I_{11/2}$ steady-state fluorescence spectra at room temperature were measured by exciting the samples with a cw Ti-sapphire ring laser at 802 nm in resonance with the $^4I_{9/2}\rightarrow{}^4F_{5/2},{}^2H_{9/2}$ absorption band. Figure 2 shows this emission for the sample doped with 1 wt% of NdF_3. The emission is inhomogeneously broadened due to site-to-site variations in the local ligand field. The fluorescence band was integrated and divided by the peak intensity to yield an effective linewidth [22]. The stimulated emission cross-section of the laser transition can be determined from spectral parameters and from the calculated radiative transition probability by making use of [22]:

$$\sigma_p\left(\lambda_p\right) = \frac{\lambda_p^4}{8\pi c n^2 \Delta\lambda_{eff}} A\left[\left({}^4F_{3/2}\right);\left({}^4I_{11/2}\right)\right] \qquad (1)$$

where λ_p is the peak fluorescence wavelength, n is the refractive index, $\Delta\lambda_{eff}$ is the effective linewidth of the $^4F_{3/2}\rightarrow{}^4I_{11/2}$ transition, and $A[(^4F_{3/2});(^4I_{11/2})]$ is the radiative transition probability for this transition. The radiative lifetime and the stimulated emission cross-section for the $^4F_{3/2}\rightarrow{}^4I_{11/2}$ transition are presented in Table 1 together with the effective fluorescence linewidth and peak position for the sample doped with 1 wt%. The sample doped with 2 wt% shows similar values for the peak position, linewidth, and stimulated emission cross-section. The stimulated emission cross-section in this fluorotellurite glass is in the range of the values found in tellurite glasses (3.0-5.1 pm^2) [14] and is similar to that found in binary zinc tellurite glasses [20, 21].

#185214 - $15.00 USD Received 11 Feb 2013; revised 4 Apr 2013; accepted 4 Apr 2013; published 8 Apr 2013

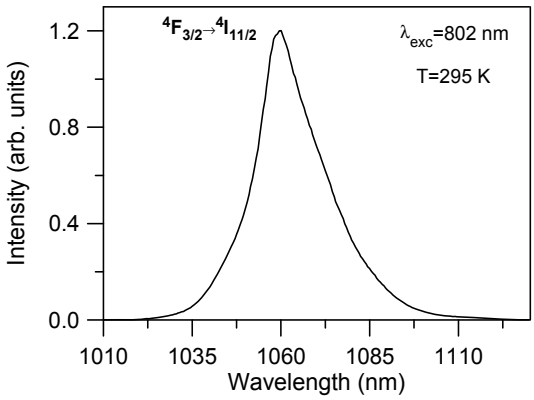

Fig. 2. Room temperature emission spectrum of the $^4F_{3/2}\rightarrow{}^4I_{11/2}$ transition of Nd^{3+} ions in TeO_2-ZnO-ZnF_2 glass doped with 1 wt% of NdF_3 obtained under excitation at 802 nm.

Table 1. Room temperature emission properties of Nd^{3+} in TeO_2-ZnO-ZnF_2 glass doped with 1 wt% of NdF_3

n	λ_p (nm)	$\Delta\lambda_{eff}$ (nm)	σ_p (x10^{-20} cm^2)	τ_R (μs)	τ_{exp} (μs)
2.064	1059	25	4.9	145	128

The decays of the $^4F_{3/2}$ state were obtained by exciting with a pulsed Ti-sapphire laser at 802 nm in the $^4I_{9/2}\rightarrow{}^4F_{5/2}$ absorption band at 295 K. Figure 3 shows the logarithmic plot of the experimental decays of the $^4F_{3/2}$ level for the samples doped with 1 and 2 wt% of NdF_3 at room temperature. As can be seen, the decay of the sample doped with 1 wt% is nearly single exponential whereas the decay of the sample doped with 2 wt% deviates from a single exponential at short times and the lifetime decreases from 128 to 90 μs as NdF_3 concentration increases from 1 to 2 wt% respectively. The lifetime value for the sample doped with 2 wt% corresponds to the average lifetime defined by $\langle\tau\rangle = \int_0^\infty tI(t)dt \Big/ \int_0^\infty I(t)dt$ where I(t) is the intensity at time t [23]. According to the value of the radiative lifetime the quantum efficiencies ($\eta = \tau_{exp}/\tau_R$) are around 88 and 62% for samples doped with 1 and 2 wt% respectively. This reduction of the quantum efficiency as concentration increases indicates the presence of non-radiative processes. The decay time from level $^4F_{3/2}$ should be the sum of probabilities from radiative and nonradiative decays by multiphonon relaxation and by energy transfer to other Nd^{3+} ions. Multiphonon relaxation is expected to be small because of the energy gap between $^4F_{3/2}$ and $^4I_{15/2}$ levels and the values of the phonon energy involved (≅750 cm^{-1}) [17]. The non-exponential character of the decays and the reduction of the lifetimes as concentration increases can be due to cross-relaxation processes such as ($^4F_{3/2}$, $^4I_{9/2}$)→ ($^4I_{15/2}$, $^4I_{15/2}$).

The analysis of the experimental decays of the sample doped with 2 wt% of NdF_3 shows that the nonradiative processes correspond to a direct transfer between Nd^{3+} ions. In this case, under the assumption of a dipole-dipole interaction, the donor decay curves can be accurately described by expression [24]:

$$I(t) = I_0 \exp\left(-\frac{t}{\tau_R} - \gamma\sqrt{t}\right) \tag{2}$$

where τ_R is the radiative lifetime of donor ions and γ characterizes the direct $Nd^{3+}\rightarrow Nd^{3+}$ energy transfer. In the case of dipole-dipole interaction, γ is given by the expression, $\gamma = \frac{4}{3}\pi^{3/2} N C_{DA}^{1/2}$, where N is the Nd^{3+} concentration and C_{DA} is the energy transfer

#185214 - $15.00 USD Received 11 Feb 2013; revised 4 Apr 2013; accepted 4 Apr 2013; published 8 Apr 2013

microparameter. In this case, the donors and acceptors are the Nd^{3+} ions. Figure 4 shows a least square fit of the experimental decay for the sample doped with 2 wt% of NdF_3 at room temperature. The obtained value for the interaction parameter C_{DA} is $5.5x10^{-40}$ cm^6/s, which is higher than those reported in fluoroindogallate ($1.3x10^{-40}$) [25] and tellurite glasses ($3.3x10^{-40}$) [26] and similar to that found in multicomponent tellurite glasses ($5.5x10^{-40}$) [27]. The critical radius R_0, which is defined as the distance at which the probability of the cross-relaxation process becomes equal to the intrinsic decay rate of the metastable level, can be calculated in terms of C_{DA} and τ_R from $R_0^6 = \tau_R C_{DA}$ which yield a value of 6.5 Å in this glass. The γ value for the sample doped with 1 wt% obtained from the fit to Eq. (2) is 26 $s^{-1/2}$, about half the one obtained for the sample doped with 2 wt% (54 $s^{-1/2}$), thus supporting the dipole-dipole transfer hypothesis.

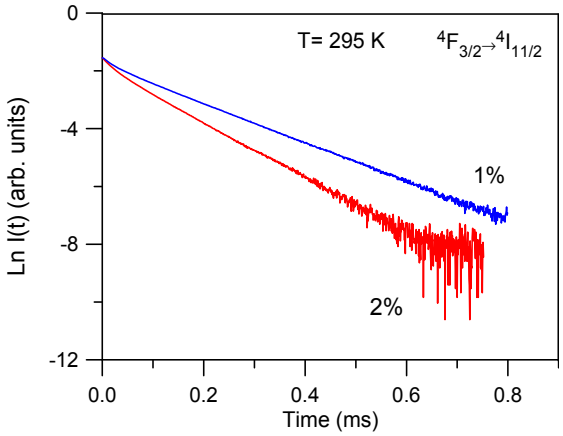

Fig. 3. Logarithmic plot of the experimental decays from the $^4F_{3/2}$ state for the samples doped with 1 wt% and 2 wt% of NdF_3. The decays were obtained by exciting at the $^4I_{9/2}\rightarrow{}^4F_{5/2}$ transition and monitored at 1059 nm. Measurements correspond to room temperature.

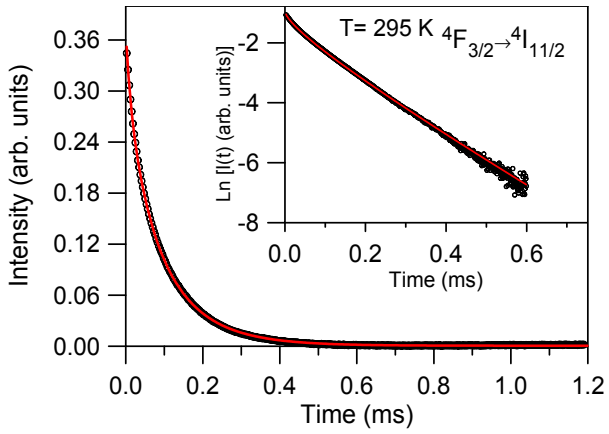

Fig. 4. Experimental emission decay curve of level $^4F_{3/2}$ and the calculated fit using Eq. (2) (solid line) for the sample doped with 2 wt% of NdF_3. The inset shows the same decay in a semilogarithmic plot.

3.2 Site-selective spectroscopy

As it is well known, in glasses, due to the site-to-site variation of the local field acting on the ions, the $^4F_{3/2}\rightarrow{}^4I_{11/2}$ transition of Nd^{3+} ions can show variations in peak wavelength, linewidth, and spectral profile depending on pumping wavelength. Therefore, selective

#185214 - $15.00 USD Received 11 Feb 2013; revised 4 Apr 2013; accepted 4 Apr 2013; published 8 Apr 2013

excitation of Nd^{3+} by changing the wavelength of the pump laser provides an additional means of varying the gain profile and affecting the laser operation. To obtain information about the crystal field site inhomogeneity of Nd^{3+} in this fluorotellurite glass we have performed low temperature site-selective spectroscopy by using a cw Ti-sapphire ring laser with a narrow bandwidth (0.4 cm^{-1}) as excitation source for the $^4I_{9/2} \rightarrow {}^4F_{3/2}$ transition. Figure 5 shows the low temperature (10 K) excitation spectra of the $^4I_{9/2} \rightarrow {}^4F_{3/2}$ transition obtained by collecting the luminescence at different wavelengths along the $^4F_{3/2} \rightarrow {}^4I_{11/2}$ transition for the sample doped with 1 wt%. As expected, these spectra show two main broad bands associated with the two Stark components of the $^4F_{3/2}$ doublet. However, the low energy component corresponding to the $^4I_{9/2} \rightarrow {}^4F_{3/2}$ doublet, narrows and blue-shifts from around 874 nm to 869 nm as the emission wavelength decreases from 1100 to 1045 nm. In addition, at some emission wavelengths, at least two components are observed. This behavior is a consequence of contributions from Nd^{3+} ions in a multiplicity of environments.

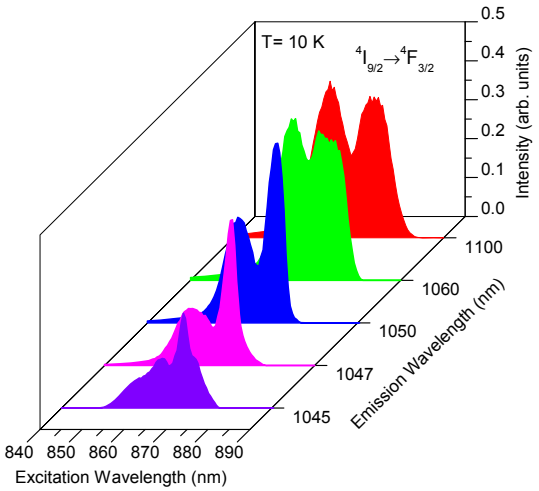

Fig. 5. Excitation spectra of the $^4I_{9/2} \rightarrow {}^4F_{3/2}$ transition obtained by collecting the luminescence at different emission wavelengths along the $^4F_{3/2} \rightarrow {}^4I_{11/2}$ emission for the sample doped with 1 wt% of NdF_3. Data correspond to 10 K.

The site-selective steady-state emission spectra of the laser transition were obtained at low temperature for different excitation wavelengths along the low energy component of the $^4F_{3/2}$ level. As can be observed in Fig. 6 the shape, peak position, and linewidth of the emission band, change with the excitation wavelength. The spectra obtained under excitation at the low energy side of the $^4I_{9/2} \rightarrow {}^4F_{3/2}$ absorption band narrow and red shift. The wavelength of the fluorescence peak shifts from 1055 to 1064 nm by varying the excitation wavelength from 870.5 to 881 nm whereas the effective linewidth is reduced from about 24 nm to 13 nm. Similar variations in fluorescence profile, peak position, and linewidth have been observed in phosphate glasses [28].

These results show the inhomogeneous behavior of the crystal field felt by Nd^{3+} ions in this fluorotellurite glass. As can be seen in Fig. 6, only when we excite at the high energy side of the absorption band it is possible to cover the full spectral range of the Nd^{3+} emission probably helped by vibronic transitions. This inhomogeneous behavior is related with the influence of the pumping wavelength on the spectral behavior of the laser emission allowing some tunability of the laser emission as a function of the pumping wavelength.

#185214 - $15.00 USD Received 11 Feb 2013; revised 4 Apr 2013; accepted 4 Apr 2013; published 8 Apr 2013

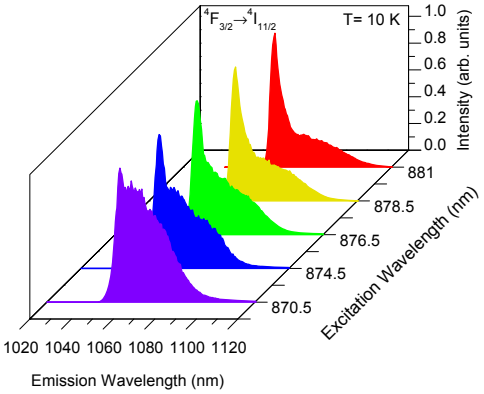

Fig. 6. Steady-state emission spectra of the $^4F_{3/2}\rightarrow{}^4I_{11/2}$ transition for different excitation wavelengths along the low Stark component of the $^4F_{3/2}$ level for the sample doped with 1 wt% of NdF_3. Data correspond to 10 K.

3.3 Laser experiments

In order to investigate the laser emission of Nd^{3+} in this glass, we have pumped the $^4F_{5/2}$ level, around 800 nm, with a pulsed Ti-sapphire laser of 0.1 nm spectral width and 10 ns pulse width. The samples were plates, with two polished faces and thicknesses of 2 and 4 mm, and NdF_3 concentrations of 1 wt% and 2 wt%. To avoid thermal damage, the sample was put out of the pump focus, being the pumping beam diameter on the sample approximately 1.2 mm. A quasi confocal symmetrical resonator was built using two concave and HR mirrors of 50 cm of curvature radius at a distance of 40 cm each other, in a longitudinal pumping scheme. In order to minimize the intra-cavity losses, the sample was placed at the center of the resonator and oriented at Brewster angle with respect to the resonator axis. The output laser pulses spectra were recorded with a diode-array Hamamatsu-Triax 190 spectrum analyzer using a 1200 lines/mm diffraction grating, whereas the temporal evolution of both the pumping and laser output was recorded by detecting the radiation diffused by the sample with a fast photodiode (rise and fall times less than 300 ps) connected to a digital oscilloscope.

Laser emission was obtained when the pump energy was above the threshold value of 27 mJ for the sample of 1% and 4 mm thickness, and slightly higher for the other thickness and concentration. This fact can be related to the relatively high absorption and possible defects concerning the optical quality of the samples. The observed delay time between pump and output laser was in the 1 μs range for the different samples and pumping levels, and the temporal width of the obtained laser pulses was about 250 ns, as can be seen in Fig. 7.

We can estimate the stimulated emission cross-section from threshold measurements and optical density measurements using the expression [28]

$$\sigma_{em} = \frac{D_0}{0.43 E_{th}\left(1-10^{-D}\right)} \tag{3}$$

where E_{th} is the threshold pump energy in photons per unit area, D is the optical density of the lasing sample over background at pump wavelength, and D_0 is the background optical density (reflectivity discounted) at the emission wavelength, which measures its optical quality. We have obtained a value of $4\text{x}10^{-20}$ cm^2 for the stimulated emission cross-section, which is higher than the ones obtained by other authors in tellurite glasses [9] and in fairly good agreement with the value obtained from the absorption and emission data (Table 1)

#185214 - $15.00 USD Received 11 Feb 2013; revised 4 Apr 2013; accepted 4 Apr 2013; published 8 Apr 2013

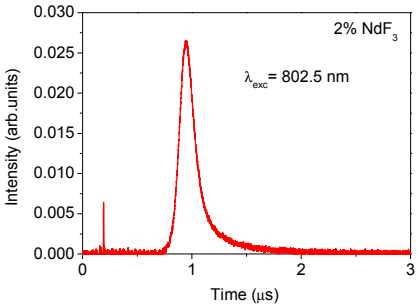

Fig. 7. Stimulated emission output pulse around 1059 nm when pumped with 30 mJ at 802.5 nm for the sample doped with 2 wt%. The small spike around 200 ns is a fraction of the pump pulse.

The laser output spectra were recorded as a function of pumping wavelength along the $^4I_{9/2}\rightarrow{}^4F_{5/2}$ absorption band. As can be seen in Fig. 8 stimulated emission occurs around 1059 nm and the maximal output intensity is achieved when pumped at 802 nm.

As an example Fig. 9 shows three series of laser emission spectra obtained at different excitation wavelengths for the sample doped with 1 wt% of NdF_3. The lowest emission peak wavelength, situated around 1058.5 nm, was obtained by exciting around 800 nm. The maximal output energy is obtained by pumping at 802 nm, which corresponds to the maximum of the absorption band. For longer pumping wavelengths, up to 805 nm, the wavelength of the emission peak shifts to higher values ranging from 1058.5 to 1061 nm. However, for excitation wavelengths longer than 806 nm, the emission peak slightly shifts again to shorter wavelengths. This behavior has also been observed in phosphate glasses [28] and attributed to the existence of well defined inhomogeneous Nd^{3+} site distributions. On the other hand, the spectral effective linewidth of the laser emission varies from 1.5 to 3.1 nm in the 1 wt% NdF_3-doped sample, showing the high crystal field inhomogeneity of the glass matrix.

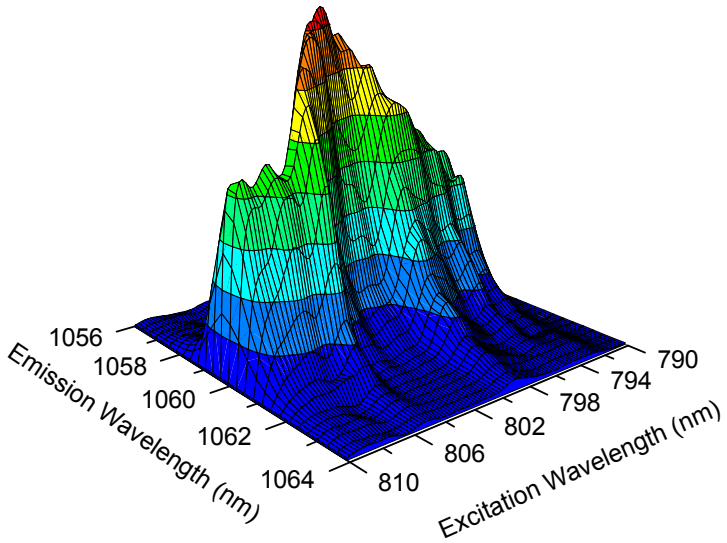

Fig. 8. Laser emission of $^4F_{3/2}\rightarrow{}^4I_{11/2}$ transition as a function of excitation and emission wavelengths for the sample doped with 1 wt%.

#185214 - $15.00 USD Received 11 Feb 2013; revised 4 Apr 2013; accepted 4 Apr 2013; published 8 Apr 2013

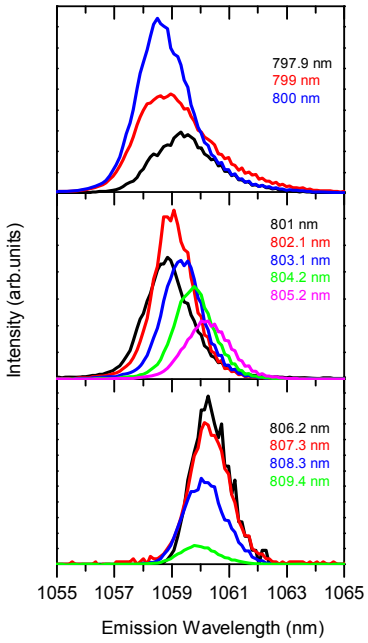

Fig. 9. Laser output spectra of $^4F_{3/2} \rightarrow {}^4I_{11/2}$ transition as a function of excitation wavelength for the sample doped with 1 wt%.

The spectral behavior of the stimulated emission under wavelength selective pumping follows similar trends to those of the spontaneous emission under wavelength selective pumping. However, the tunability of the emission peak for the stimulated emission occurs in a shorter range due to gain limitations.

4. Conclusions

Absorption and luminescence measurements have been performed in TeO_2-ZnO-ZnF_2 fluorotellurite glass doped with 1 and 2 wt% NdF_3 by using steady-state and time-resolved laser spectroscopy. The JO intensity parameters and radiative transition probabilities have been calculated. The stimulated emission cross-section for the laser transition calculated from spectral data gives a value of 4.9×10^{-20} cm^2 in reasonably good agreement with the value estimated from laser threshold data (4×10^{-20} cm^2). The time evolution of the decays from state $^4F_{3/2}$ is consistent with a dipole-dipole direct energy transfer mechanism.

The site-selective emission and excitation spectra show the inhomogeneous behavior of the crystal field felt by Nd^{3+} ions in this fluorotellurite glass. This is related with the influence of the pumping wavelength on the spectral behavior of the laser emission which allows for spectral tuning of the laser output as a function of the pumping wavelength.

The relatively high value of the stimulated emission cross-section of the laser transition suggests that these glasses are promising laser materials. Though the high value of both linear and nonlinear refractive indices can produce self focusing, and becomes a handicap for laser operation, this drawback may be overcome by using these glasses in fiber and waveguide devices.

Acknowledgments

This work was supported by the Spanish Government MEC under Projects No. MAT2009-14282-C02-02, MAT2009-14282-C02-01, FIS2011-27968, Consolider SAUUL CSD2007-00013, and Basque Country Government (IT-659-13 and SAIOTEK S-PE12UN016).

#185214 - $15.00 USD Received 11 Feb 2013; revised 4 Apr 2013; accepted 4 Apr 2013; published 8 Apr 2013